



Since January 2020 Elsevier has created a COVID-19 resource centre with free information in English and Mandarin on the novel coronavirus COVID-19. The COVID-19 resource centre is hosted on Elsevier Connect, the company's public news and information website.

Elsevier hereby grants permission to make all its COVID-19-related research that is available on the COVID-19 resource centre - including this research content - immediately available in PubMed Central and other publicly funded repositories, such as the WHO COVID database with rights for unrestricted research re-use and analyses in any form or by any means with acknowledgement of the original source. These permissions are granted for free by Elsevier for as long as the COVID-19 resource centre remains active.

Cell proliferation and apoptosis in rat mammary cancer after electrochemical treatment (EChT)

H. von Euler^{a,*}, K. Stråhle^b, A. Thörne^{c,1}, G. Yongqing^{b,2}

^aFaculty of Veterinary Medicine, Department of Small Animal Clinical Sciences, Swedish University of Agricultural Sciences (SLU), P.O. Box 7037, S-750 07 Uppsala, Sweden

^bDepartment of Microbiology, Pathology and Immunology, Division of Pathology, Huddinge University Hospital, Karolinska Institutet, S-141 86 Stockholm, Sweden

^cDepartment of Surgery, Huddinge University Hospital, Karolinska Institutet, S-141 86 Stockholm, Sweden

Received 16 June 2003; received in revised form 25 August 2003; accepted 10 October 2003

Abstract

Background: Several authors have recently reported encouraging results from Electrochemical treatment (EChT) in malignant tumours. However, EChT is not established and mechanisms are not completely understood. In vivo studies were conducted to evaluate the toxic changes and effectiveness of EChT on an animal tumour model. **Methods:** Tumours were induced by injecting cells from the R3230AC rat mammary tumour cell line clone D subcutaneously, in 28 female Fischer 344 rats. EChT was conducted by inserting a platinum electrode into the tumours. The positive and negative control groups were subjected to the same conditions but without current. The rats were kept for 0, 7 or 14 days post-treatment. Three hours prior to euthanasia an i.p. injection of Bromodioxuryridine (BrdU) was given. The rats were euthanized, the lesions extirpated and samples were collected for histopathological, and immunohistochemical examination. **Results:** Significant changes in cell proliferation rate were seen both in the cathode and anode regions. Apoptosis were induced in the anodic treated area outside the primary necrosis, detected with the TUNEL method. **Discussion:** The results suggest that secondary cell destruction was caused by necrosis with cathodic EChT and apoptosis or necrosis with anodic EChT.

© 2003 Elsevier B.V. All rights reserved.

Keywords: Electrochemical treatment (EChT); Tumour; Rat; Apoptosis; pH

1. Introduction

Electrochemical treatment (EChT) of tumours has been used for more than a hundred years [1]. Although treated with great concern, during the last years many encouraging reports have been published where authors report of tumour destruction in a wide range of tumour models like subcutaneous sarcomas [2], melanomas [3], intramuscular implanted hepatomas [4], subcutaneous Lewis lung carcinoma [5] and most recently in liver tumours [6,7].

Electrolysis is a simple technique using a direct current passed through a conductive medium between a pair of electrodes, measured in Coulombs ($1\text{ C} = 1\text{ A} \times 1\text{ s}$). At the cathode (negative electrode) sodium hydroxide and hydrogen gas are liberated, whereas at the anode (positive electrode), hydrochloric acid, oxygen, and chlorine gas are produced [8,9]. The resulting pH change, the anode becomes acidic relative to the basic environment surrounding the cathode, causes a localised parenchymal necrosis [10,11]. The electric field causes a flux of interstitial water, electro-osmosis, from the anode towards the cathode, since the water molecules act like a dipole. Consequently, the tissue surrounding the anode dehydrates while oedema is obtained around the cathode [9,12]. Charged substances, dissolved or suspended in tissue, migrate in the electric field and accumulation of ions and charged tissue constituents are obtained at certain and different locations in the electric field. The electric field influences the ion exchange across the cell membranes. Hence, the transmembrane potential is

* Corresponding author. Tel.: +46-18-67-13-63; fax: +46-18-67-35-34.

E-mail address: henrik.von.euler@kirmed.slu.se (H. von Euler).

¹ Present address: Department of Surgery, Södertälje Hospital, S-152 86 Södertälje, Sweden.

² Present address: Department of Thoracic Surgery, China–Japan Friendship Hospital, Beijing 100029, People's Republic of China.

altered and thereby the conditions, e.g. for many essential enzyme-regulated reactions [9,13]. There is a negligible thermal effect [14].

The clinical introduction of EChT has been hindered by uncertainty regarding dose planning and mechanisms of destruction. In 1983 Professor Nordenström reported results from the treatment of 26 lung tumours in 20 patients [9]. Many of these patients were, for various reasons, unsuitable for surgical, radiotherapeutic or chemotherapeutic treatment. Regression was obtained in 12 out of 26 tumours and no signs of re-growth were detected after a 2–5 year follow-up period. Among the side effects, Nordenström noticed slight fevers and local pain during the treatment. From the early 1990s until today more than 15 000 patients have been treated with EChT in China [15]. The results have been presented in a number of publications and at several conferences and have been thoroughly reviewed, for example by Nilsson et al. [16]. Despite the vast experiences from China and recent clinical experimental studies in Australia [17] EChT is still not established and obviously endorse the need for further investigation concerning e.g. destructive mechanisms.

Here we present a suitable experimental model to evaluate the mechanism and effectiveness of low-level direct current therapy in mammary carcinoma in rat, with the R3230AC mammary carcinoma model, first described by Hilf et al. [18].

In a previous work we were able to identify, *in vitro*, the effect of a pH gradient on the tumour cell line used in the animal model [19]. The aim of this study was to see if similar results regarding cell morphology, proliferation and induction of apoptosis could be achieved after EChT *in vivo* and if any differences between the electrode polarity, coulomb given and duration after treatment could be detected. In addition it was investigated if an indication of destructive efficacy could be obtained.

2. Materials and methods

The animal experiments conformed fully to the Swedish Animal Ethical Committee's code S84/00.

The inoculation model was performed as earlier described by Sapino et al. [20] with some slight modifications.

2.1. Cell line and culture methods

The R3220AC rat mammary tumour cell line (clone-D; kindly provided by Prof. G. Bussolati, University of Turin, Italy) was cultured in RPMI 1640 with Glutamax I medium (GIBCO™, Invitrogen, Stockholm, Sweden) supplemented with 10% heat-inactivated foetal bovine serum and plated in tissue culture flasks (Falcon Plastics, Los Angeles, CA) in a humidified 37 °C, 5% CO₂ incubator. When the cells reached approximately 80% confluence, they were collected by trypsin-EDTA treatment. Briefly the cellsheet was rinsed

once with Ca²⁺- and Mg²⁺-free PBS and incubated for approximately 5 min at 37 °C in the presence of fresh trypsin-EDTA. After incubation the cells were suspended in RPMI 1640 for injection. Viability was determined for harvested cell batches using the trypan blue exclusion dye method. All cells used for this study showed >90% viability.

2.2. Animals and tumour induction

Tumours were induced by injecting 0.5 ml (0.5–0.8 × 10⁶ cells) R3230AC Rat mammary tumour clone D subcutaneously into the shaved left and right region 1 cm caudal to the scapula in rats weighing 185–210 g. Before the tumour model was commenced a test inoculation performed at the The National Veterinary Institute (SVA, Uppsala, Sweden) on SPF rats had proven that the clone D were free from the following viruses; Murine Poliovirus/Theiler's encephalomyelitis virus (TEV), Reovirus type 3, Hantaan virus, Parainfluenza virus type 1 (PMV-1)-Sendai, Pneumonia virus of mice (PVM), Rat coronavirus and Parvovirus/Kilham rat viruses (KRV). The procedure of subcutaneous implantation was performed under aseptic conditions. The animals were divided into two dose categories (10 or 20 C; C=A s) with a follow up period after treatment of 0, 7 or 14 days. Each group consisted of four rats. Moreover, nine positive controls (tumour cells inoculated and electrodes inserted but no electric treatment; three rats for each time period) and three negative controls; one for each time period (as for pos controls but only RPMI 1640 injected) were included in the study, making the total number of rats 36. Animals were kept under defined flora conditions in our animal facility. They were allowed food and water *ad libitum*.

Tumours size measurements were made using a digital Vernier calliper. The three longest, orthogonal diameters (*a*, *b* and *c*) were registered. Tumour volume was calculated using the formula ($\pi abc/6$). Tumours were allowed to grow for approximately 21 days, which resulted in nodules that had a mean volume ± SD of 416 ± 382 mm³. Tumours were elevated above the skin and easily measured with a digital Vernier calliper (Guanglu, Taizhou, China). The rats were treated under general anaesthesia using midazolam (Dormicum®, Roche, Stockholm) 1.2 mg/ml and fentanyl-fluanisone (Hypnorm®, Janssen Animal Health, Buckinghamshire, UK) diluted 1:4, which was injected *i.p.* 0.3 ml/100 g [21]. After induction, one half of the initial dose was iterated every 30 min. A heating gel pillow was placed underneath the animal to avoid hypothermia.

Two identical string shaped electrodes made of Pt:Ir (9:1), with a diameter of 0.5 mm, were used throughout the experiments. The string was electrically insulated using Teflon®, despite the active electrode, 10 mm long. Before each use, the electrodes were disinfected in 70% ethanol. The electrodes were placed in the left and right tumour, through a small cutaneous incision and were held firmly by a supporting gantry. The electrodes were inserted in a

caudal-cranial direction with the rats in ventral recumbency lying on their chest. In all procedures, the electrode on the animal's right was made anodic. The electrode spacing varied between 15 and 25 mm.

Direct current was passed through the electrodes by means of a constant-current power supply, consisting of a potentiostat (Wenking LT 73, Germany) coupled to an adjustable resistance. The current and voltage were continually monitored with multimeters (3610D METEX® Instru-Instruments, Korea), and data was recorded on a Palm pilot IIIx® (Palm, Santa Clara, CA, USA) using the accompanying software (Quickoffice, Cutting Edge Software, USA). To avoid muscle twitching, linear current ramps with a length of 2 min were used to reach the current level (10 mA) and before turning off at the end of the treatment. The total coulomb was continually calculated and the treatment was interrupted when a total dose of 10 or 20 C had been delivered. The applied voltage automatically varied in the range of 0–20 V throughout the treatment, since the equipment was designed to maintain a constant current.

After EChT, rats were returned to the animal housing facility. The rats were wrapped in heat insulating towels and housed separately when waking up, to optimise postoperative recovery and to prevent cannibalising one another's tumours; later on four rats were housed per cage. During the first 24 h postoperatively the rats received two i.p. injections of Buprenorphine (Temgesic®, Schering-Plough AB, Stockholm, Sweden) 0.05 mg/kg to sustain accurate analgesia. Tumour wounds were inspected daily.

After treatment the animals' status was continuously examined. 3 h prior to euthanasia the rats were given an i.p. injection of 5-Bromo-2'-deoxyuridine (BrdU) 100 mg/kg, dissolved in sterile, 0.9% sodium chloride.

The rats were euthanized by administering 3 ml Na-pentobarbital 2.5% i.p., the lesions extirpated and samples were collected for histopathological and immunohistochemical examination. Sample buffer used was 4% phosphate buffered formaldehyde.

2.3. Histopathological and immunohistochemical examination

2.3.1. Morphology

The tissue was examined in a light microscope (Nikon ECLIPSE E 1000) after staining with haematoxylin eosin according to routine procedures. For investigation of potential distant metastases, tissue from liver, spleen and lungs were examined.

2.3.2. Cell proliferation

For the immunohistochemical quantification of cell proliferation the S-phase marker BrdU (thymidine analogue) was used. After dewaxing the paraffin sections in xylene and rehydrated in ethanol according to standard procedures, the slides were rinsed and kept in TBS for at least 15 min. The glasses were placed in a beaker with 0.01 M citrate

buffer pH (6.0), heated to boiling point in a microwave oven and then kept boiling for 10 min. The buffer and tissue sections were cooled down to room temperature during 20 min in cold water. To block endogenous peroxidase activity the sections were incubated with 0.75% H₂O₂ solved in methanol for 30 min in RT. The sections were rinsed in tap water and subsequently with TBS 2 × 5 min. To improve antibody penetration the sections were treated with 0.1% protease in TBS for exactly 5 min in RT, followed by careful rinsing with TBS for 15 min. To block unspecific binding the sections were incubated with 5% BSA-TBS for 15 min, then covered with the primary antibody (mouse anti-BrdU, Dako, Glostrup, Denmark) for 1 h in RT. After careful washing, the secondary antibody (rabbit anti-mouse biotinylated, Dako) was applied to the sections and incubated for 30 min before it was removed with TBS. Thereafter the Avidine–Biotin–Complex /HRP (Dako) was added and rinsed off after 30 min, followed by DAB (diaminobenzidine, Sigma) staining for 7 min. Counterstaining with Hematoxylin (Mayer, Merck) for 5 min was performed according to conventional procedures. Finally, the sections were rinsed in tap water for approximately 10 min. Dehydration and mounting followed standard routines.

The labelling index (LI), the ratio of BrdU positive cells and the total amount of cells, was quantified by light microscopy. Seventy high power fields were examined in each section. The counting started at the border of the primary destruction caused by heavily pH changes[10], in this paper called the border of destruction and moved out towards untreated tumour tissue in a sunray pattern, with the electrode as the centre. The cumulative incidence of BrdU

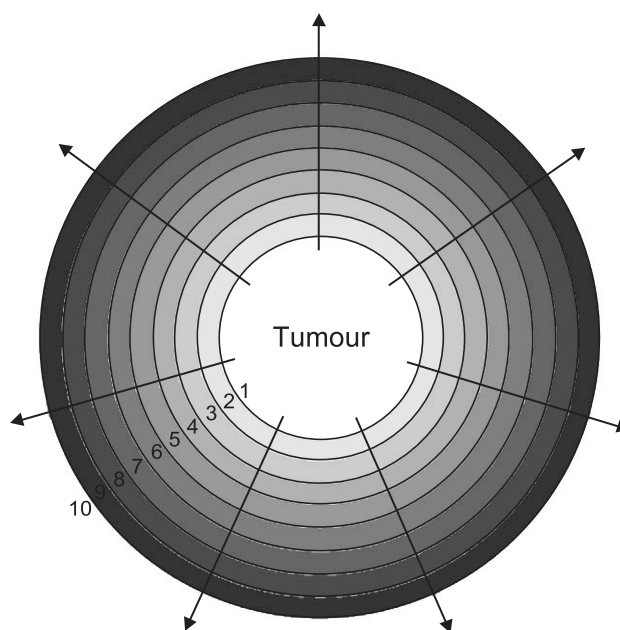


Fig. 1. A schematic of how the cell proliferation labelling index (LI) was determined. In the seven directions indicated by the arrows each of the zones numbered 1 through 10 was evaluated, starting at the border of destruction (zone 1).

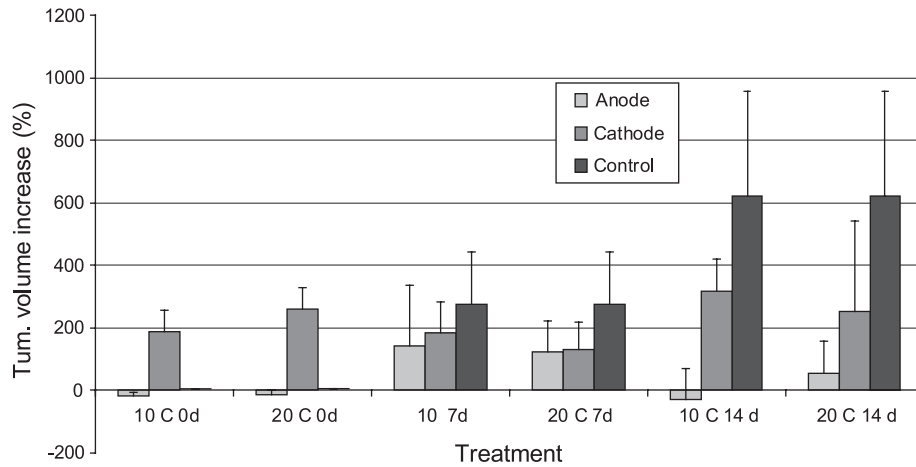


Fig. 2. Average tumour size after EChT compared to untreated control. In the beginning the anodic treatment gives rise to an immediate decrease in tumour volume due to dehydration. At day 0 the initial tumour volume and the one after treatment is the same for the control. Hence, the difference in volume becomes 0. There is an illusory prominent increase in “tumour volume” immediately after EChT at the cathode due to the formation of oedema (electro-osmosis). Error bars are showing the standard deviation (SD), which is the percentage increase/decrease from start of the experiment (e.g. day 21) until termination (0, 7 or 14 days after EChT).

labelled cells was determined for each of the ten high power fields, called zones, counted (Fig. 1). In the positive control the counting started at the border of the central necrosis, spontaneously formed in the tumour.

2.4. TUNEL

For the immunohistochemical detection and quantification of apoptosis (programmed cell death) at single cell

level, based on labelling of DNA strand breaks (TUNEL technology) the In Situ Cell Death Detection Kit, POD (Roche Diagnostics, Mannheim, Germany) was used. The formalin-fixed tissue sections were dewaxed and transferred into PBS. After incubation with proteinase K 20 µg/ml in 10 mM Tris–HCl for 20 min in 37 °C the slides were rinsed in PBS 2 × 5 min, followed by blocking the endogenous peroxidase activity with 3% H₂O₂ in methanol for 10 min in RT. After additional rinsing in PBS 2 × 5 min the slides

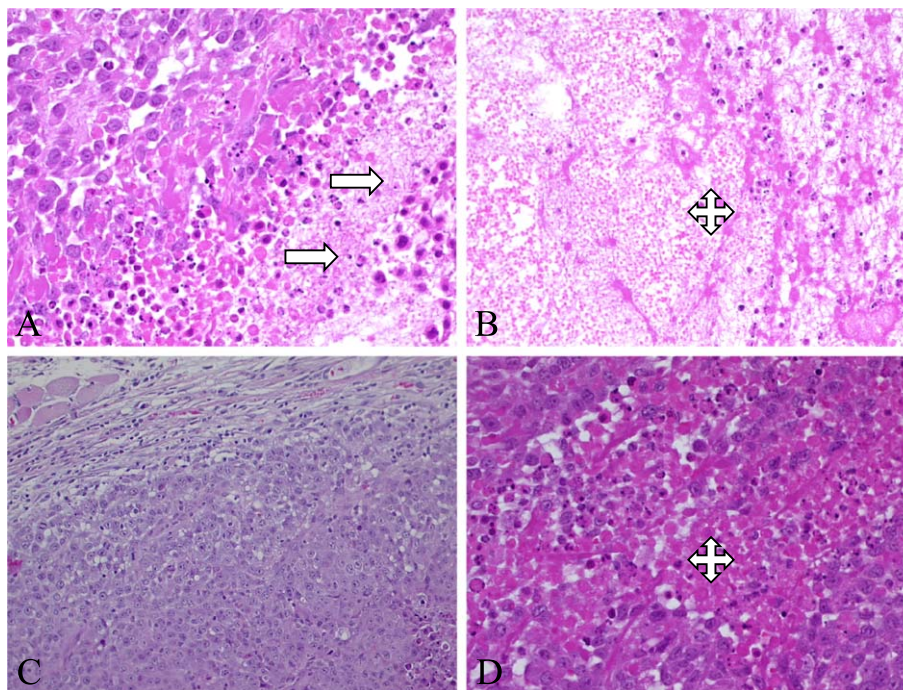


Fig. 3. Histopathological examination of the R3230AC Rat mammary tumour clone D after EChT. At the anodic treatment (20 C 7d) the border of destruction is clearly visible (A, magnification 212 ×) and a marked central necrosis has developed with a secondary inflammation (B, magnification 212 ×). The untreated control has a prominent capsule (C, magnification 100 ×) and contains a few minor local necroses (D, magnification 212 ×). Arrows marking the area of necrosis.

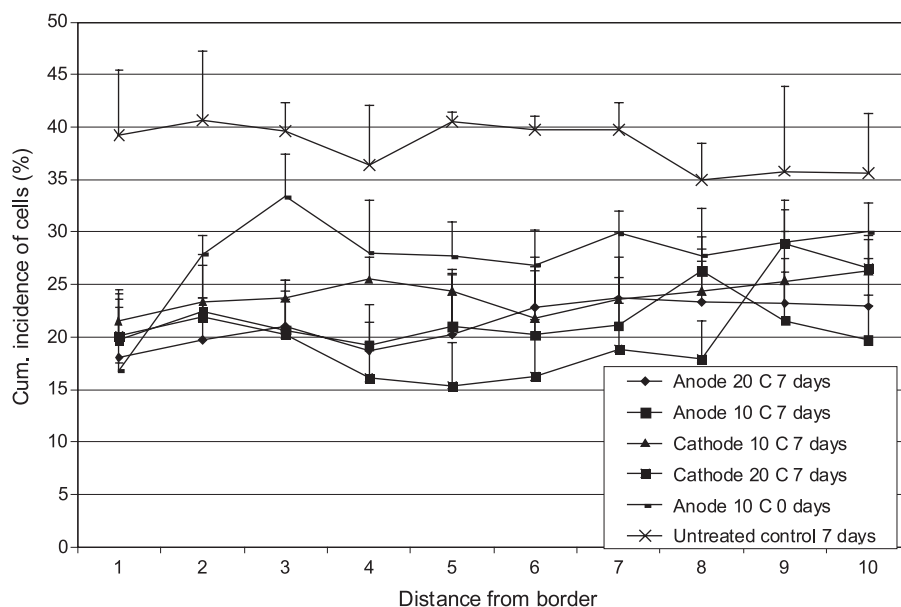


Fig. 4. Chart showing the cumulative incidence of tumour cells in S-phase from the border of destruction and out towards “normal” tumour tissue. Note that the cell proliferation is significantly decreased even far from the actual EChT destruction, suggesting that additional impact on tumour proliferation is achieved, apart from the primary necrosis. Initially (0d) the decrease in cell proliferation rate is more prominent close to the border of destruction, due to toxic impact from the produced hydrochloric acid, oxygen, and chlorine gas (anode) or sodium hydroxide (cathode; not shown). Further away from the necrotic area it becomes higher than for the 7d group. Error bars are showing the standard deviation (SD).

were incubated in permeabilisation solution 0.1% Triton X-100 (Sigma) in 0.1% sodium citrate (Merck) for 2 min in 4 °C. After rinsing in PBS at RT, 50 µl of TUNEL reaction mixture was added on the section and incubated for 60 min at 37 °C in a humidified atmosphere in the dark. After rinsing the slides in PBS, samples were analysed in a fluorescence microscope (Leica TCS NT ArKr laser confocal microscope). For light microscope analysis 50 µl Converter-POD was added on the samples followed by incubation in a humidified chamber for 30 min at 37 °C. After rinsing slides in PBS, 100 µl DAB-substrate solution (Roche Diagnostics) was added. A final 10 min incubation at RT followed. After the last rinse with PBS the slides were counterstained with Haematoxylin (Merck) and mounted according to standard routines. Subsequently analysis in a light microscope (Nikon ECLIPSE E 1000 with a SONY 3 CCD color video camera) was performed.

2.5. Statistics

Tumour volumes were expressed as mean \pm standard deviation (SD). Data were analysed as a mixed model according to Littell et al. [22] using the individual animal as a random factor. Time and anode, cathode or none were used as fixed factors. The procedure Mixed in the SAS package was used for the analysis [23]. A *p*-value of less than 0.05 was considered statistically significant. The comparison of the proliferation rate, with immunohistochemistry, between the therapeutic and the control group was statistically analysed with the Student's *t*-test. A *p*-value of less than 0.05 was considered statistically significant.

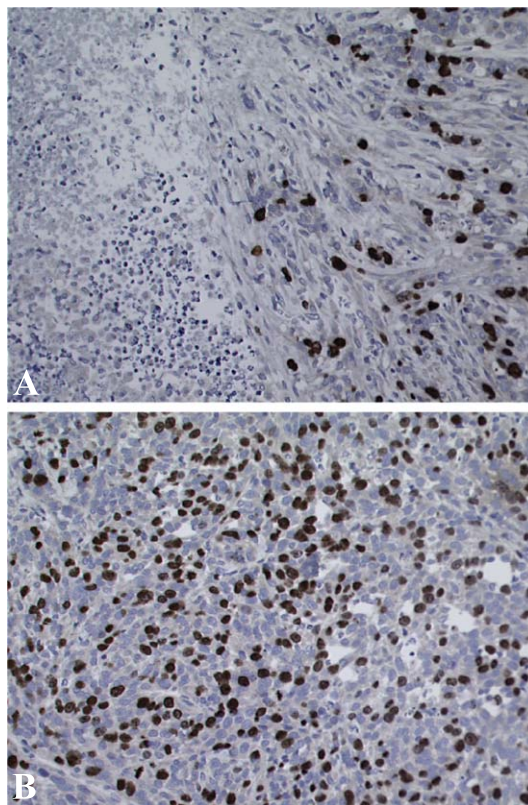


Fig. 5. Cell proliferation after EChT. Ten high power fields were counted in the light microscope after staining for BrdU incorporation (brown nuclei). Note the decrease in proliferation far from the border of destruction in the cathodic treatment (A, magnification 212 \times) compared to the untreated control (B, 212 \times).

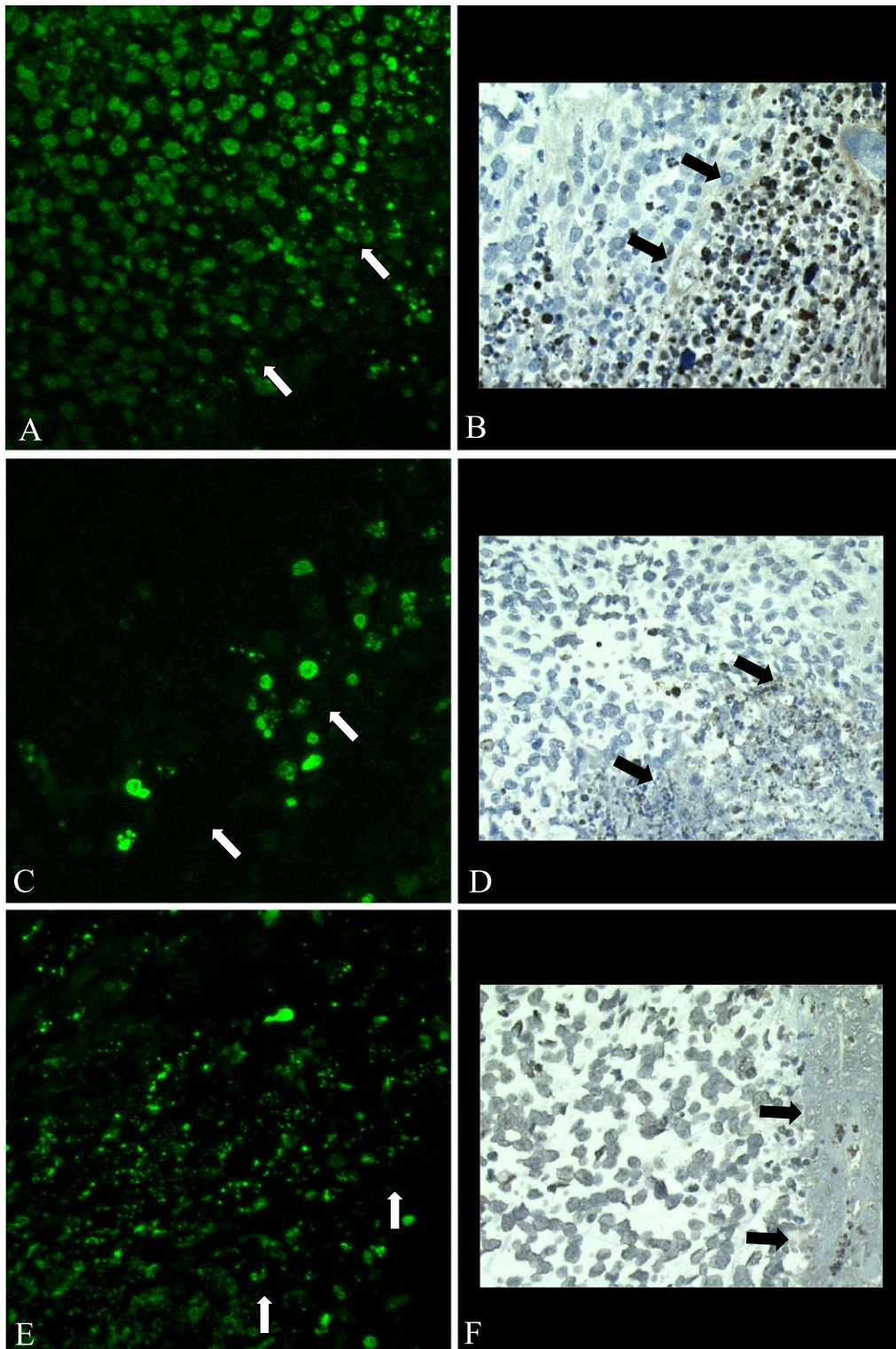


Fig. 6. Immunohistochemistry using the *TUNEL* method shows the induction of apoptosis after EChT (10 C 7d). In fluorescence microscope the distinct apoptotic nuclei at the border of destruction at the anode (A, objective $64\times$) is compared to the untreated control (C, objective $64\times$) where few apoptotic nuclei are found and the cathodic treatment (E, objective $64\times$) where a general necrosis is present. After staining with peroxidase technique the apoptosis can be seen in the light microscope (B, D and F; magnification $212\times$). The light microscope view is placed beside the corresponding immunofluorescence picture. Arrows mark the border of destruction or necrotic margin.

3. Results

The initial volumes of tumours were $416 \pm 382 \text{ mm}^3$. The difference (percentage) between the tumour volume initially and after 0, 7 and 14 days post treatment, respectively, were assessed by means of comparing the mean difference for each treatment group, divided with the initially determined tumour volume. Hence, the variation in initial tumour volume, between groups, could be neglected (Fig. 2).

After the EChT was supplied to tumours, it was observed that the volumes initially decreased at the anode and increased at the cathode when compared with the control. Only one rat went into complete remission (Anode 10 C, 7d). The tumour sloughed off 4 days after EChT. In the rest a significant decrease (both anode and cathode) in tumour progression compared to untreated control was achieved. Significant tumour responses were found in the anode 10 C 14d and 20 C 14d, when compared to the corresponding cathodic treatments as well as the controls.

3.1. Histopathological examination

Tumour cells were easily identified on hematoxylin and eosin sections by their basophilic properties and polymorph appearance. The tumours were well delimited and did seldom attach to underlying muscles. Tumour samples, positive control and treated (anode) are shown in Fig. 3. Microscopic examination of the control group indicated that the mammary tumours that developed showed the characteristics, described in detail by Papotti et al. [24], of a high differentiated solid adenocarcinoma with minor central necroses.

The necrosis surrounding the positive electrode was coagulative in nature with preservation of the architectural contours. In contrast, the necrotic areas surrounding the negative electrode exhibited liquefaction and almost complete effacement of tissue architecture (not shown).

Due to the subtotal tumour destructive dose, in all cases except the complete remission described earlier, necroses and reparative tissue were found alongside remnants of vital tumour conglomerates. The necrotic areas occurred mostly as coagulation necroses in organization, interspersed with connective tissue. The necrotic area was sharply demarcated from the adjacent tumour. Several necroses were partially encased in vital tumour tissue. Distant metastases were not detected in any of the inoculated rats following macroscopic as well as microscopic examination of lung, spleen and liver tissue. This confirms the findings of a former study by Sapino et al. [20].

3.2. Cell proliferation

There was a significant decrease in cell proliferation both at the anode and cathode compared to the positive control. The labelling index (LI) was almost constant from the

border of destruction and further out in less affected tumour tissue. An example of this is shown for animals killed 7 days after EChT (Fig. 4). The positive control can be compared to the significantly decreased BrdU labelling for both anode (not shown) and cathode treatments (Fig. 5). Cell proliferation was significantly impaired far from the macroscopic as well as microscopic visible border of destruction. Initially (0d) the proliferation rate was significantly decreased close to the border of destruction, for both 10 C and 20 C, compared to the 7d and 14d post EChT groups (all groups not shown). Further out from the necrotic area the 0d-group had a higher LI instead, compared to the other treatments. 10 C (0d) is included in Fig. 4.

3.3. Apoptosis

The spontaneous amount of apoptosis in the R3230AC Rat mammary tumour cell line is very low in vitro [19]. After EChT an induction of apoptosis was found in the anodic treated areas at the border of destruction compared to both the untreated control as well as the cathode groups. In fluorescence microscope (Fig. 6) the light green stained nuclei express the presence of cleaved genomic DNA that during apoptosis have yield doublestranded, low molecular weight DNA fragments (mono- and oligonucleosomes) as well as single strand breaks (“nicks”) in high molecular weight DNA. Labelling free 3' -OH termini with modified nucleotides in an enzymatic reaction can identify those DNA strand breaks. In the cathode treatments very necrotic material was found close to the destruction zone and almost no intact nuclei were considered as being apoptotic. In the controls the general frequency of apoptosis was investigated, especially at the border of the spontaneous central necrosis/necroses. Occasionally, clusters of positive stained cells were found, but the overall amount of apoptosis was low. In the light microscope the findings in the fluorescence microscope were confirmed (Fig. 6).

4. Discussion

This subtotal tumour destruction trial was carried out to investigate the possible biological features of EChT on mammary carcinomas and not being a treatment modality for dose–response calculations. Hence, the dose could be sustained at a low level, minimising the postoperative trauma and patient discomfort. Despite the large variation in initial tumour size and small number of animals, it was possible to prove a statistical difference between the untreated control and the rats that underwent EChT, even if this was not the primary aim of this study.

The single electrode configuration also made it possible to separately examine the different polarities' influence on the tumour, still working in the same individual. As we believe that the pH alterations during EChT is the major reason for tissue destruction we have recently presented a

paper where the R3230AC Rat mammary tumour clone D was investigated *in vitro* [19]. In this study tumour cells were exposed to a pH gradient similar to that of EChT and after a variable period of recovering in normal medium investigations were carried out concerning viability (MTT-test), morphological observation in phase contrast microscope and light microscope, nucleotide analogue incorporation (BrdU), caspase-3 activity measurement and detection of DNA fragmentation by an agarose gel electrophoresis. In this study cell proliferation was significantly impaired, both in acidic and alkaline milieu. More interesting however was the fact that apoptosis was induced only in strong acidic environment and that the cell morphology distinctly resembles the features seen in *in vivo* experiments with EChT.

Since the induction of apoptosis is concentrated to the border of destruction at the anode the most probable mechanism is the acidification that occurs. This is also supported by the *in vitro* study described above. Interestingly the cell proliferation rate was reduced significantly in the whole tumour, both for the anodic and cathodic treatment, suggesting that secondary mechanisms such as the inflammatory response, tumour ischemic anoxia and radical formations also impair the tumour progression after EChT. Hence, the treatment had a significant effect on tumour cells proliferation far from the evidently destroyed area.

Very few studies with EChT have separated the two electrodes and studied the different impact on the cell damage. In this trial an excellent possibility to study this was achieved. The information could be useful if it is known that a specific tumour is more prone to resist, or susceptible to undergo, apoptosis. The choice of tumour may influence the treatment outcome and could possibly explain why different studies have claimed either the anode or the cathode as being more efficacious.

The direction of the intracellular pH (pH_i) change (acidification or alkalinisation) as well as the level of the change depends on the extracellular (pH_e). It is well known that acute extracellular acidification acidifies the intracellular environment, thereby perturb the cell proliferation [25]. Low pH_e results in low pH_i because of increased H^+ entry. Intracellular acidification correlates well with DNA digestion, and acidic cells show apoptotic morphology [26]. It has also been shown that acid endonuclease can be responsible for the DNA cleavage seen in apoptotic neutrophils [27]. Thus, acidification is a potential signal for the final, irreversible stages of cell death.

The destructive mechanism in higher pH is that alkalic condition directly destroy various enzyme and structure proteins and result in inactivation of function or protein denaturation. Intracellular alkalinisation increases the inward calcium current and the resultant increase of intracellular Ca^{2+} [28]. The initiating event in necrosis leads to an influx of water and extracellular ions. Intracellular organelles, most notably the mitochondria, and eventually the entire cell, swell and rupture, the structure of the relatively unchanged DNA is randomly degraded.

EChT perturbs blood perfusion in treated tumours and thus leads to growth retardation [29,30]. It is also described that EChT causes micro thrombi that eventually lead to ischemic injury [9,17]. It is however not clear if there is any difference between electrode polarities, considering micro thrombi formation and hypoxic lesions, although some reports claim a slightly stronger impact at the anode [31,32]. Apoptosis is triggered by a hypoxic environment [33,34]. Thus, it is easy to assume that the apoptosis found in this study is due to ischemic injury. However, it is hard to explain why there is such a difference between the anodic and cathodic treatments. Furthermore, the results in the previous described *in vitro* study support the hypothesis that low pH induces apoptosis, whereas high pH induce necrosis [19]. Taking these two studies together they indicate that the EChT of R3220AC cells and exposition of low pH *in vitro* exhibit several features of apoptosis including chromatin condensation, DNA fragmentation, TUNEL labelling and activation of caspases.

The observations in the animal model can certainly be a combination of both acidic milieu and hypoxia, although most likely with low pH as the predominating factor.

The development of different EChT treatment modalities is getting increasing interest in the Western world. Basic investigations of the cellular behaviour in both normal and neoplastic tissue are good complements to the large-scale models and long terms studies of the safety effects of electrochemical treatment that recently have been published [6,35,36]. The introduction of EChT as a complement in the treatment of tumours in humans as well as companion animals can soon be anticipated.

Acknowledgements

Professor Lennart Eriksson and Associate Professor Jerker Olsson, at the Department of Microbiology, Pathology and Immunology, Division of Pathology, Huddinge University Hospital, are acknowledged for being scientific advisors and for histopathological consultation.

Ulf Olsson, Associate Professor, Department of Biometry and Informatics, SLU, Uppsala, is acknowledged for statistical consultation.

This work was in part financially supported by the AGRIA-insurance company Stockholm, Sweden.

References

- [1] T. Cavallo, A complete treatise on electricity in theory and practice, Dilly, London, 1777.
- [2] C.E. Humphrey, E.H. Seal, Biophysical approach toward tumor regression in mice, *Science* 130 (1959) 388–390.
- [3] M.K. Schauble, M.B. Habal, H.D. Gullick, Inhibition of experimental tumor growth in hamsters by small direct currents, *Arch. Pathol. Lab. Med.* 101 (1977) 294–297.

- [4] M.B. Habal, Effect of applied dc currents on experimental tumor growth in rats, *J. Biomed. Mater. Res.* 14 (1980) 789–801.
- [5] D.M. Morris, A.A. Marino, E. Gonzalez, Electrochemical modification of tumor growth in mice, *J. Surg. Res.* 53 (1992) 306–309.
- [6] S.A. Wemyss-Holden, G.S. Robertson, P.M. Hall, A.R. Dennison, G.J. Maddern, Electrolytic treatment of colorectal liver tumour deposits in a rat model: a technique with potential for patients with unresectable liver tumours, *Dig. Dis.* 18 (2000) 50–57.
- [7] A. Turler, H. Schaefer, N. Schaefer, D. Maintz, M. Wagner, J.C. Qiao, A.H. Hoelscher, Local treatment of hepatic metastases with low-level direct electric current: experimental results, *Scand. J. Gastroenterol.* 35 (2000) 322–328.
- [8] L. Samuelsson, L. Jonsson, Electrolyte destruction of lung tissue. Electrochemical aspects, *Acta Radiol., Diagn. Stockh.* 21 (1980) 711–714.
- [9] B.E. Nordenström, *Biologically Closed Electric Circuits: Clinical, Experimental and Theoretical Evidence for an Additional Circulatory System*, Nordic Medical Publications, Stockholm, 1983.
- [10] H. von Euler, E. Nilsson, A.-S. Lagerstedt, J.M. Olsson, Development of a dose-planning method for electrochemical treatment of tumors. A study of mammary tissue in healthy female CD-rats, *Electro-Magneto-biol.* 18 (1999) 93–105.
- [11] J.G. Finch, B. Fosh, A. Anthony, E. Slimani, M. Texler, D.P. Berry, A.R. Dennison, G.J. Maddern, Liver electrolysis: pH can reliably monitor the extent of hepatic ablation in pigs, *Clin. Sci. (Lond.)* 102 (2002) 389–395.
- [12] A.K. Vijn, Electrochemical treatment of tumors (ECT): electroosmotic dewatering (EOD) as the primary mechanism, *Drying Technol.* 17 (1999) 585–596.
- [13] L. Vodovnik, D. Miklavcic, G. Sersa, Modified cell proliferation due to electrical currents, *Med. Biol. Eng. Comput.* 30 (1992) 21–28.
- [14] D. Miklavcic, G. Sersa, M. Kryzanowski, S. Novakovic, F. Bobanovic, R. Golouh, L. Vodovnik, Tumor treatment by direct electric current—tumor temperature and pH, electrode material and configuration, *Bioelectrochem. Bioenerg.* 30 (1993) 209–220.
- [15] Y. Xin, F. Xue, B. Ge, F. Zhao, B. Shi, W. Zhang, Electrochemical treatment of lung cancer, *Bioelectromagnetics* 18 (1997) 8–13.
- [16] E. Nilsson, H. von Euler, J. Berendson, A. Thörne, P. Wersäll, I. Näslund, A.-S. Lagerstedt, K. Narfström, J.M. Olsson, Review—electrochemical treatment of tumours, *Bioelectrochemistry* 51 (2000) 1–11.
- [17] S.A. Wemyss-Holden, A.R. Dennison, G.J. Finch, P.M. Hall, G.J. Maddern, Electrolytic ablation as an adjunct to liver resection: experimental studies of predictability and safety, *Br. J. Surg.* 89 (2002) 579–585.
- [18] R. Hilf, I. Michel, G. Silverstein, G. Bell, Effect of actinomycin D on estrogen-induced changes in enzymes and nucleic acids of R3230AC mammary tumors, uteri, and mammary glands, *Cancer Res.* 25 (1965) 1854–1859.
- [19] H. von Euler, A. Söderstedt, J.M. Olsson, A. Thörne, G. Yongqing, Cellular toxicity induced by different pH levels on the R3230AC rat mammary tumour cell line. An in vitro model for investigation of the tumour destructive properties of electrochemical treatment of tumours, *Bioelectrochemistry* 58 (2002) 163–170.
- [20] A. Sapino, M. Papotti, B. Sanfilippo, P. Gugliotta, G. Bussolati, Tumor types derived from epithelial and myoepithelial cell lines of R3230AC rat mammary carcinoma, *Cancer Res.* 52 (1992) 1553–1560.
- [21] P.A. Flecknell, Anaesthesia of animals for biomedical research, *Br. J. Anaesth.* 71 (1993) 885–894.
- [22] R.C. Littell, G.A. Milliken, W.W. Stroup, R.D. Wolfinger, SAS System for Mixed Models, SAS Institute, Cary, NC, 1996.
- [23] R.D. SAS Institute, SAS/Stat User's Guide, SAS Institute, Cary, NC, 1999.
- [24] M. Papotti, R. Coda, A. Ottinetti, G. Bussolati, Dual secretory and myoepithelial differentiation in the transplantable R3230AC rat mammary carcinoma, *Virchows Arch., B Cell Pathol. Incl. Mol. Pathol.* 55 (1988) 39–45.
- [25] H.J. Park, J.C. Lyons, T. Ohtsubo, C.W. Song, Acidic environment causes apoptosis by increasing caspase activity, *Br. J. Cancer* 80 (1999) 1892–1897.
- [26] M.A. Barry, J.E. Reynolds, A. Eastman, Etoposide-induced apoptosis in human HL-60 cells is associated with intracellular acidification, *Cancer Res.* 53 (1993) 2349–2357.
- [27] R.A. Gottlieb, H.A. Giesing, R.L. Engler, B.M. Babior, The acid deoxyribonuclease of neutrophils: a possible participant in apoptosis-associated genome destruction, *Blood* 86 (1995) 2414–2418.
- [28] R.D. Smith, D.A. Eisner, S. Wray, The effects of changing intracellular pH on calcium and potassium currents in smooth muscle cells from the guinea-pig ureter, *Pflugers Arch.* 435 (1998) 518–522.
- [29] D. Miklavcic, T. Jarm, M. Cemazar, G. Sersa, D.J. An, J. Belehradec, L.M. Mir, Tumor treatment by direct electric current. Tumor perfusion changes, *Bioelectrochem. Bioenerg.* 43 (1997) 253–256.
- [30] T. Jarm, Y.A. Wickramasinghe, M. Deakin, M. Cemazar, J. Elder, P. Rolfe, G. Sersa, D. Miklavcic, Blood perfusion of subcutaneous tumours in mice following the application of low-level direct electric current, *Adv. Exp. Med. Biol.* 471 (1999) 497–506.
- [31] D.T. Griffin, N.J.F. Dodd, S. Zhao, B.R. Pullan, J.V. Moore, Low-level direct electrical current therapy for hepatic metastases: I. Pre-clinical studies on normal liver, *Br. J. Cancer* 72 (1995) 31–34.
- [32] G.S. Robertson, S.A. Wemyss-Holden, A.R. Dennison, P.M. Hall, P. Baxter, G.J. Maddern, Experimental study of electrolysis-induced hepatic necrosis, *Br. J. Surg.* 85 (1998) 1212–1216.
- [33] M. Deshmukh, Caspases in ischaemic brain injury and neurodegenerative disease, *Apoptosis* (1998) 387–394.
- [34] J.K. Brunelle, N.S. Chandel, Oxygen deprivation induced cell death: an update, *Apoptosis* 7 (2002) 475–482.
- [35] S.A. Wemyss-Holden, P.M. Hall, G.S. Robertson, A.R. Dennison, P.S. Vanderzon, G.J. Maddern, The safety of electrolytically induced hepatic necrosis in a pig model, *Aust. N.Z. J. Surg.* 70 (2000) 607–612.
- [36] S.A. Wemyss-Holden, G.S. Robertson, A.R. Dennison, P.S. Hall, P.M. Hall, G.J. Maddern, A new treatment for unresectable liver tumours: long-term studies of electrolytic lesions in the pig liver, *Clin. Sci.* 98 (2000) 561–567.